Supporting Information

Triphenylamine-functionalized luminescent sensor for efficient *p*-nitroaniline detection

Ning-Ning Ji[a], Zhi-Qiang Shi[a,c]*, Hai-Liang Hu[b]* and He-Gen Zheng[c]*

[a]*College of Chemistry and Chemical Engineering, Taishan University, Taian 271021, P. R. China.*

[b]*School of Chemical Engineering* (*School of Chinese Pharmacy*), *Guizhou Minzu University, Guiyang 550025, P. R. China.*

[c]*State Key Laboratory of Coordination Chemistry, School of Chemistry and Chemical Engineering, Collaborative Innovation Center of Advanced Microstructures, Nanjing University, Nanjing 210093, P. R. China.*

S1. Synthesis of Hbpba

Hbpba was synthesized according to the literature method with a modification as the follows.[1, 2]

Step 1: 4-(bis(4-(pyridin-4-yl)phenyl)amino)benzaldehyde was synthesized according to the literature report with a modification as follows.[1] A mixture of 4-(bis(4-bromophenyl)amino)benzaldehyde (4.31 g, 10.0 mmol), 4-pyridinylboronic acid (3.69 g, 30.0 mmol), K_3CO_3 (8.29 g, 60.0 mmol), and $Pd(PPh_3)_4$ (1.16 g, 1.0 mmol) in 200 mL of 1,4-dioxane/water (v/v = 4:3) was heated to 115 °C for 3 days under N_2 atmosphere. After cooling to room temperature, solvent was removed under reduced pressure. The organic layer was extracted with $CHCl_3$ (150 mL × 3). The organic layer was dried by anhydrous $MgSO_4$ and filtered. The solvent was removed under reduced pressure. The crude product was separated by silica gel column chromatography (petroleum ether/ethyl acetate = 1:1, v/v) to afford 4-(bis(4-(pyridin-4-yl)phenyl)amino)benzaldehyde as a yellow powder in a yield 3.20 g (74.9%).

Step 2: The product (2.14 g, 5.0 mmol) of the first step is dissolved in 50 mL of acetone: water (v/v = 4:1) solution. And 2.0 g $KMnO_4$ is added to the solution. During solution is refluxed, add another portion of $KMnO_4$ twice in 2 hr interval. The dark solution was filtered and the filtrate was evaporated under reduced pressure. 50 ml water was added and diluted HCl (6.0 $mol{\cdot}L^{-1}$) was dropped until pH ≈ 5. The precipitates were filtered out and washed with water several times. Dry the precipitates to afford the product 4-(bis(4-(pyridin-4-yl)phenyl)amino)benzoic acid as a yellow power in a yield 2.0 g (90.2%). ^{1}HNMR(500 MHz, DMSO): δ: 12.70 (s, 1H), 8.64 (d, 4H), 7.90 (d, 2H), 7.86 (d, 4H), 7.70 (d, 4H), 7.27 (d, 4H), 7.12 (d, 2H).

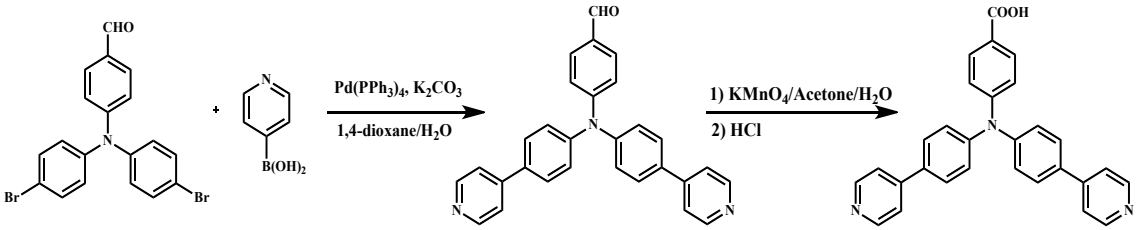

Scheme 1. Two-step synthesis route of ligand Hbpba.

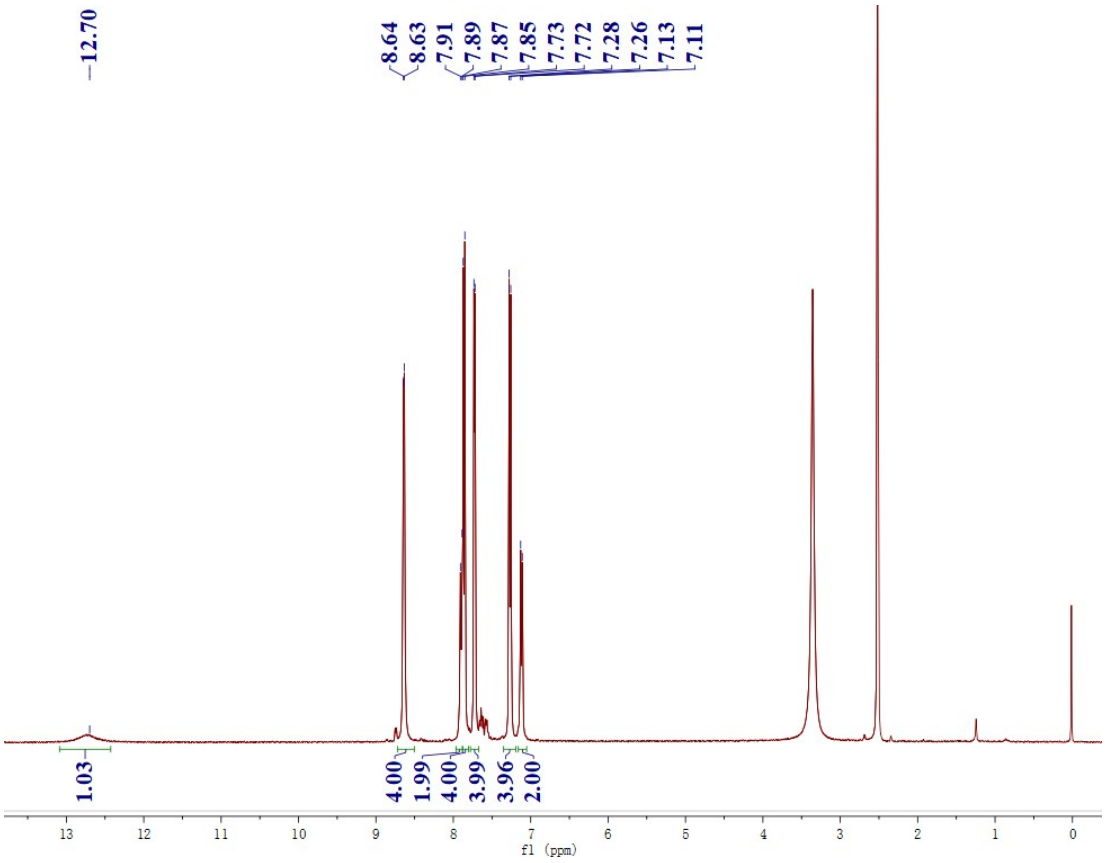

Fig. S1 ^{1}H NMR (DMSO-d_6, 500 MHz) of ligand Hbpba.

Table S1. Selected Bond Lengths (Å) and Angles (deg) for **1**.

Zn(1)-O(3)	1.974(5)	Zn(1)-N(2)	2.050(3)
Zn(1)-O(1)#1	2.003(3)	Zn(1)-N(3)#2	2.045(3)
O(3)-Zn(1)-N(2)	107.4(2)	O(3)-Zn(1)-O(1)#1	104.88(18)
O(1)#1-Zn(1)-N(2)	95.81(14)	O(1)#1-Zn(1)-N(3)#2	115.03(15)
O(3)-Zn(1)-N(3)#2	126.09(19)	N(3)#2-Zn(1)-N(2)	103.12(13)
Symmetry codes: #1 = 1.5 - *x*, -*y*, -0.5 + *z*; #2 = 1.5 - *x*, 1 - *y*, -0.5 + *z*.			

Table S2. HOMO and LUMO energies calculated for **1**, Hbpba and nitroaromatics analytes[3]

Analytes	HOMO (eV)	LUMO (eV)	Band gap (eV)
Hbpba[a]	-5.4913	-1.6096	3.8818
1[b]	-4.1743	-0.79468	3.3796
p-NA[a]	-6.1110	-1.8654	4.2456
o-NA[a]	-6.0396	-2.1636	3.8760
m-NA[a]	-5.9152	-2.1709	3.7443
p-AA[a]	-6.0034	-0.8961	5.1073
A[a]	-5.1196	-0.3785	4.7410
NB[a]	-7.5904	-2.4286	5.1617
p-AP[a]	-4.9898	-0.1227	4.8670
p-TI[a]	-4.9574	0.3921	5.3495

a: The isodensity surfaces and energy levels of the HOMO and LUMO orbitals for Hbpba and analyte molecules were calculated by density functional theory (DFT) at the B3LYP/6-31G(d) level.

b: The isodensity surfaces and energy levels of the HOMO and LUMO orbitals for **1** were calculated by density functional theory (DFT) at the B3LYP. The calculation was performed by using the LANL2DZ basis set for Zn atom and the standard 6-31G(d) for C, H, O and N atoms.

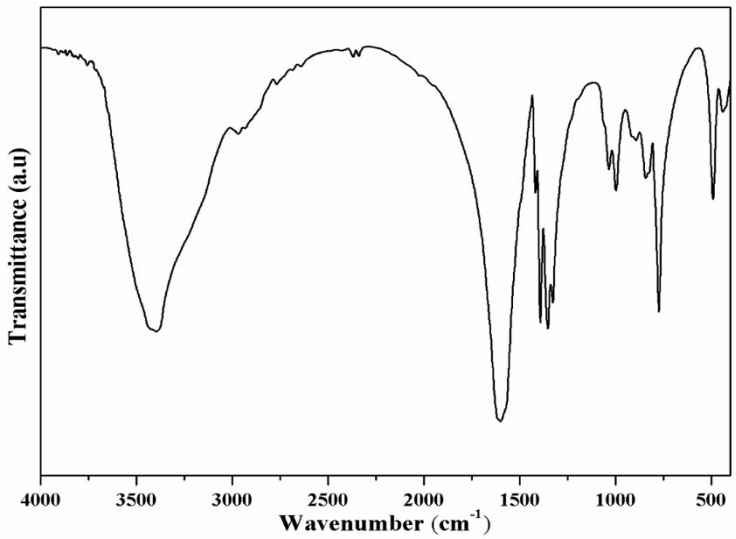

Fig. S2 IR spectra of **1**.

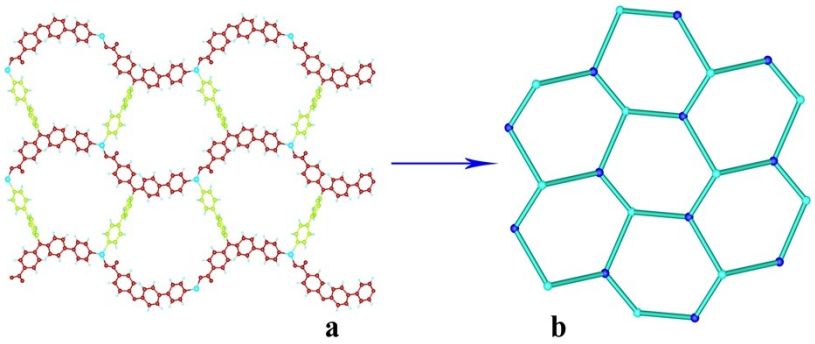

Fig. S3 Perspective view of 2D layer network (a) and (3, 3)-connected 6^3-**hcb** topology (b) of **1**.

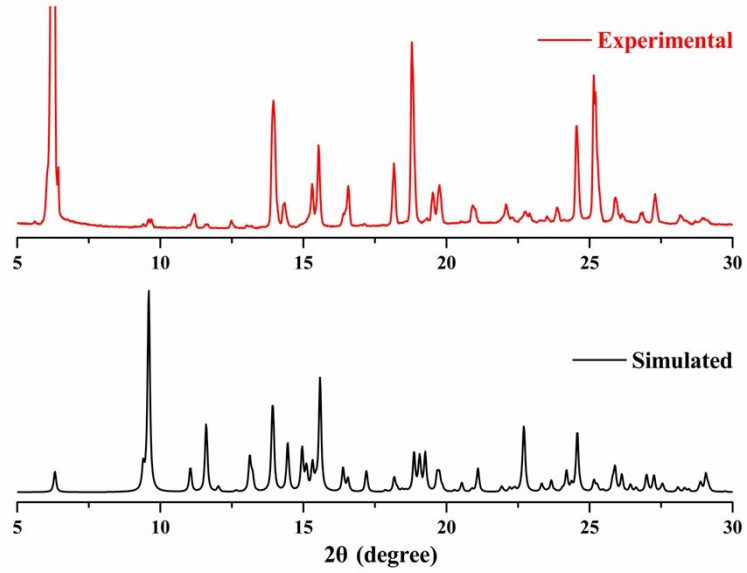

Fig. S4 Powder X-ray diffraction patterns of **1**.

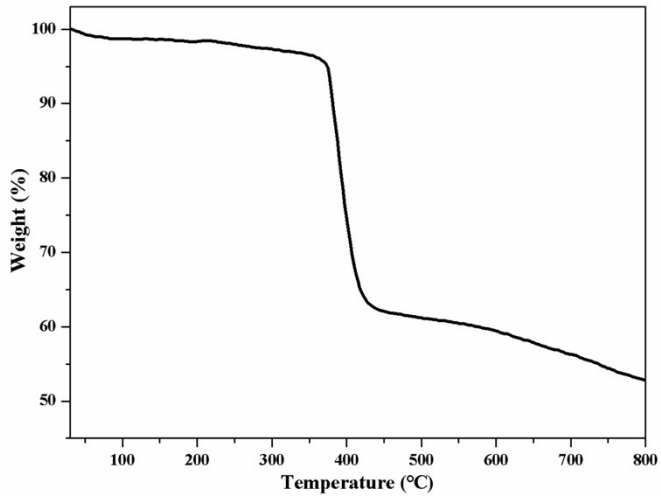

Fig. S5 TGA curve of **1**.

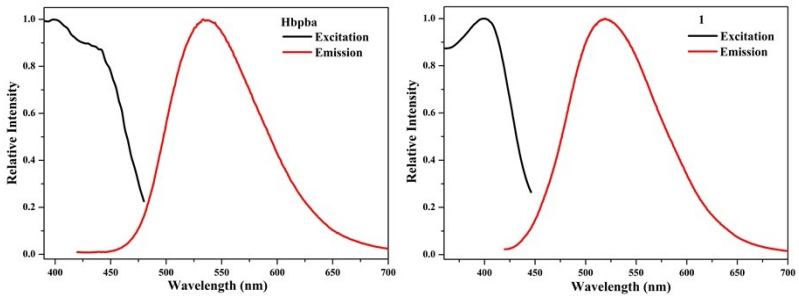

Fig. S6 Photoluminescence excitation (black curves) and emission (red curves) spectra of free Hbpba ligand and **1** at room temperature.

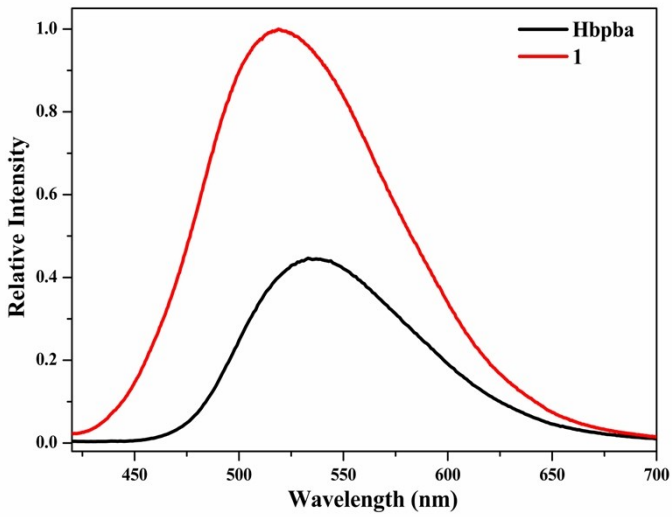

Fig. S7 The relative photoluminescence intensity of Hbpba and **1** in the solid state at room temperature.

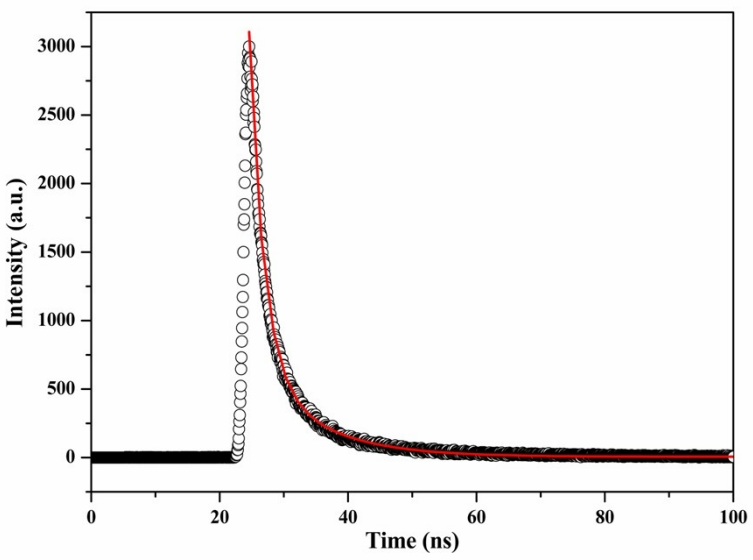

Fig. S8 The fitted decay curve monitored at 533 nm for Hbpba in the solid state at room temperature. Blank circles: experimental data; Solid line: fitted by Fit = A + B_1 × exp(-t / τ_1) + B_2 × exp(-t / τ_2).

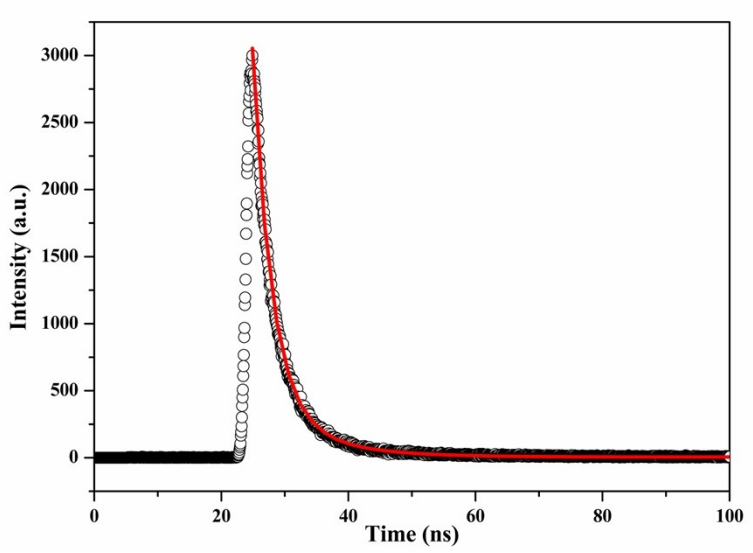

Fig. S9 The fitted decay curve monitored at 519 nm for **1** in the solid state at room temperature. Blank circles: experimental data; Solid line: fitted by Fit = A + B_1 × exp(-t / τ_1) + B_2 × exp(-t / τ_2).

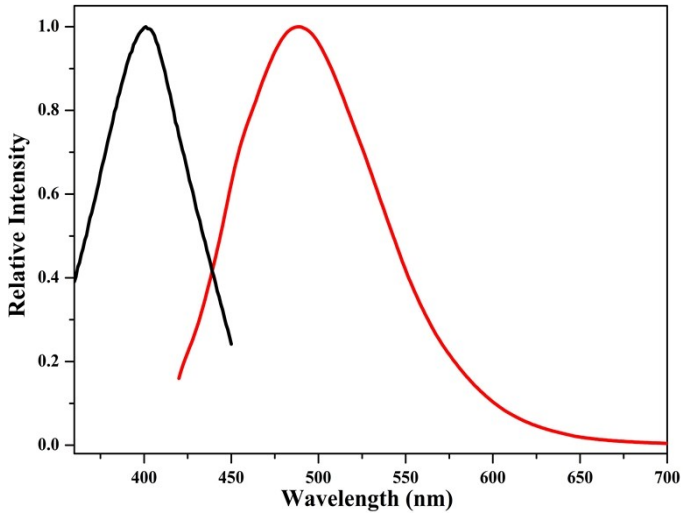

Fig. S10 Photoluminescence excitation (black curves) and emission (red curves) spectra of **1** in DMF at room temperature.

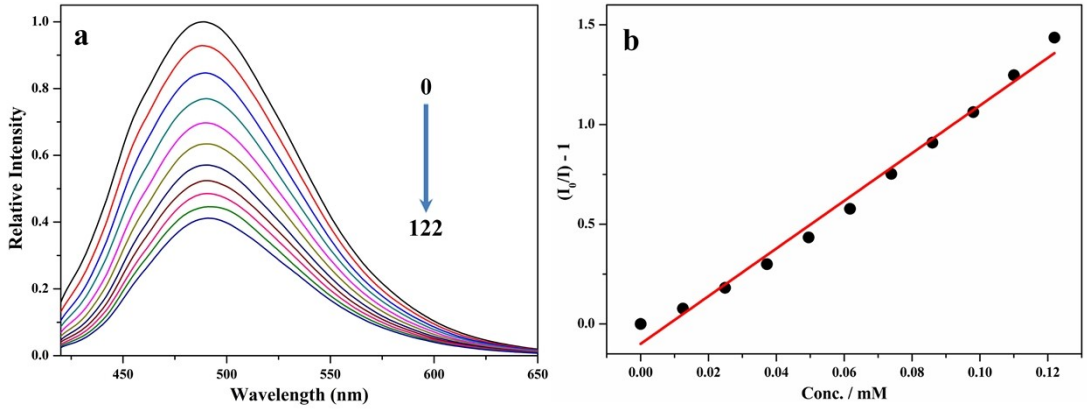

Fig. S11 Photoluminescent spectra (a) and SV plot (b) of **1** treated with *o*-NA concentration from 0 μM (black line) to 122 μM (royal line).

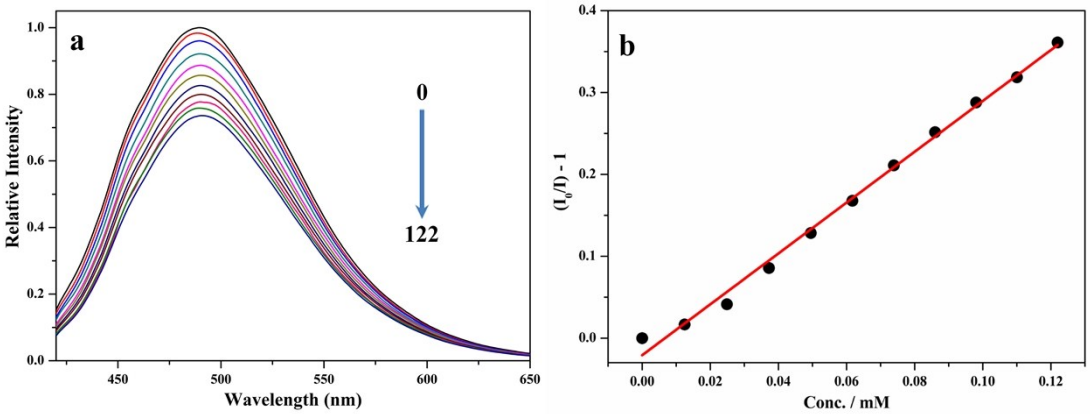

Fig. S12 Photoluminescent spectra (a) and SV plot (b) of **1** treated with *m*-NA concentration from 0 μM (black line) to 122 μM (royal line).

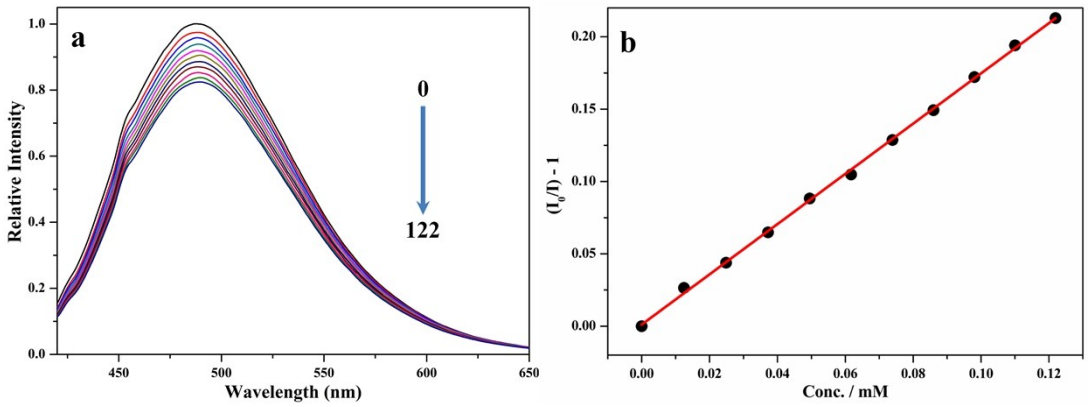

Fig. S13 Photoluminescent spectra (a) and SV plot (b) of **1** treated with A concentration from 0 μM (black line) to 122 μM (royal line).

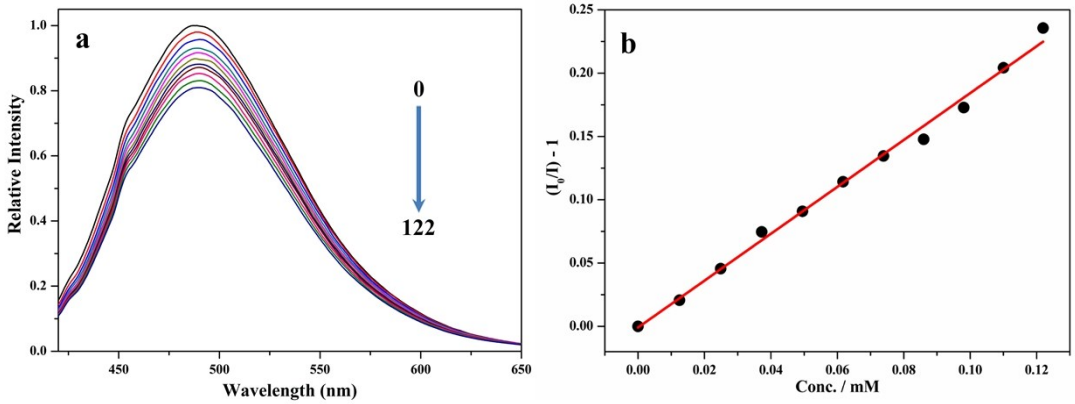

Fig. S14 Photoluminescent spectra of **1** treated with *p*-AA concentration from 0 μM (black line) to 122 μM (royal line).

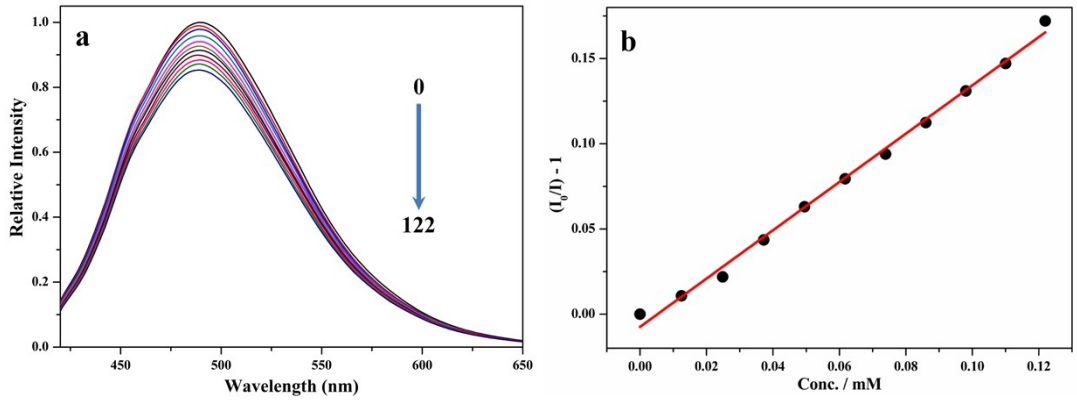

Fig. S15 Photoluminescent spectra (a) and SV plot (b) of **1** treated with *p*-TI concentration from 0 μM (black line) to 122 μM (royal line).

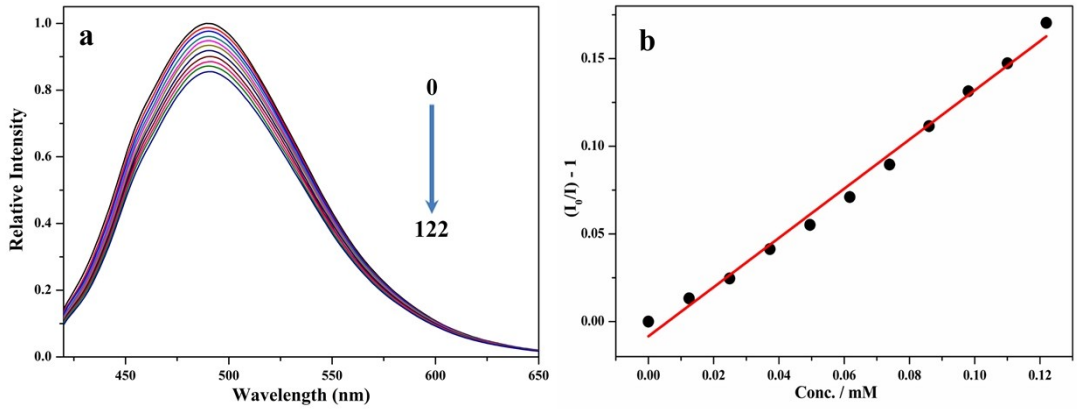

Fig. S16 Photoluminescent spectra (a) and SV plot (b) of **1** treated with *p*-AP concentration from 0 μM (black line) to 122 μM (royal line).

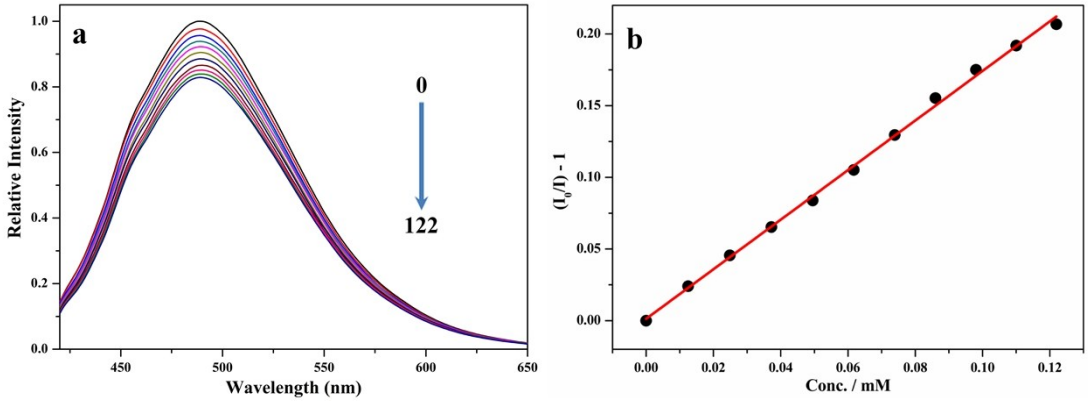

Fig. S17 Photoluminescent spectra (a) and SV plot (b) of **1** by gradual addition of 5 mM NB concentration from 0 μM (black line) to 122 μM (royal line).

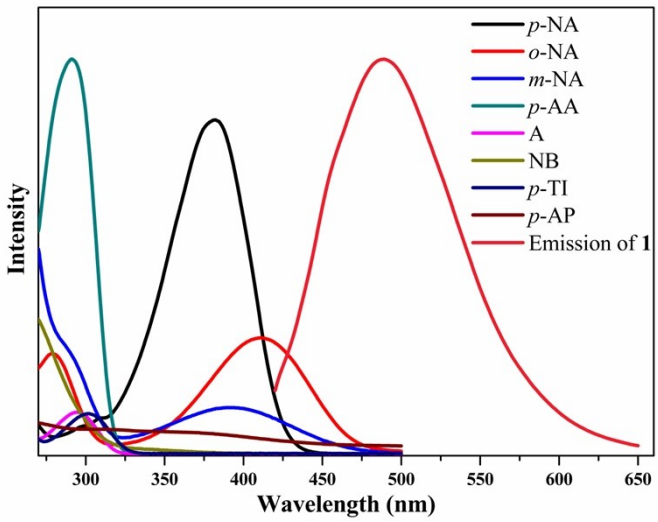

Fig. S18 Spectral overlap between normalized absorbance spectra of aromatic analytes and the normalized emission spectra of **1** in DMF.

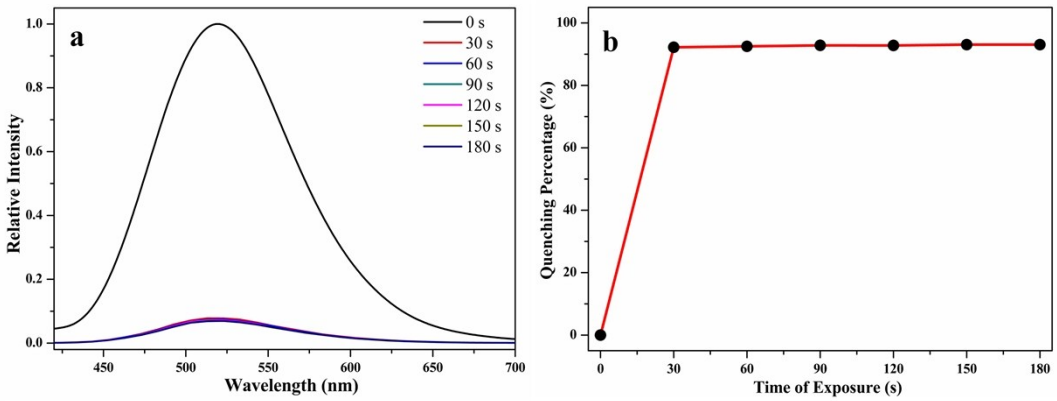

Fig. S19 Time-dependent photoluminescent spectra (a) and quenching percentage (b) of **1** to the *p*-NA vapor.

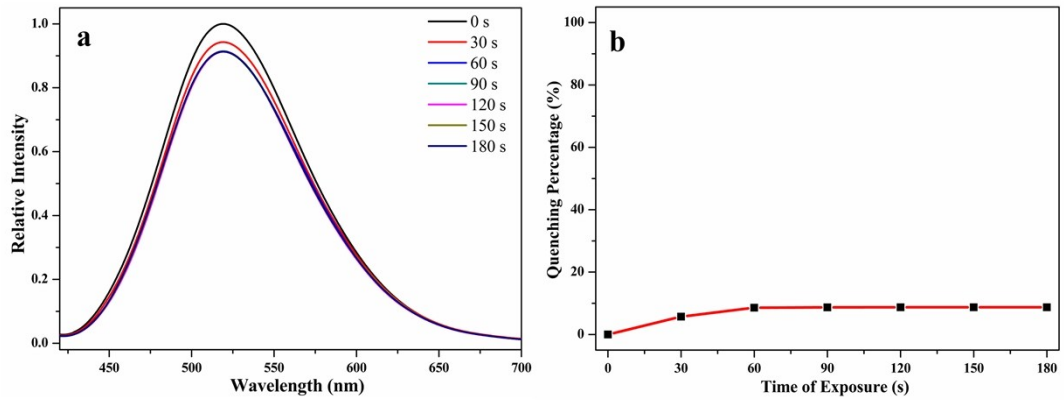

Fig. S20 Time-dependent photoluminescent spectra (a) and quenching percentage (b) of **1** to the *p*-AP vapor.

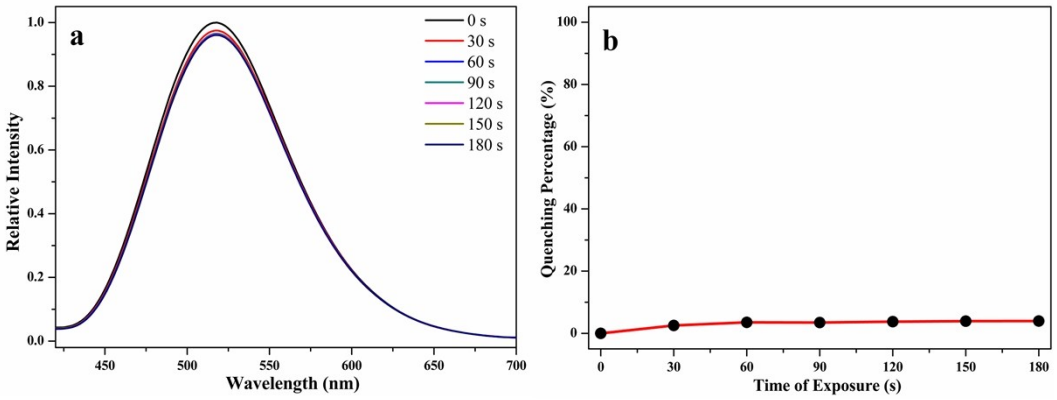

Fig. S21 Time-dependent photoluminescent spectra (a) and quenching percentage (b) of **1** to the *p*-TI vapor.

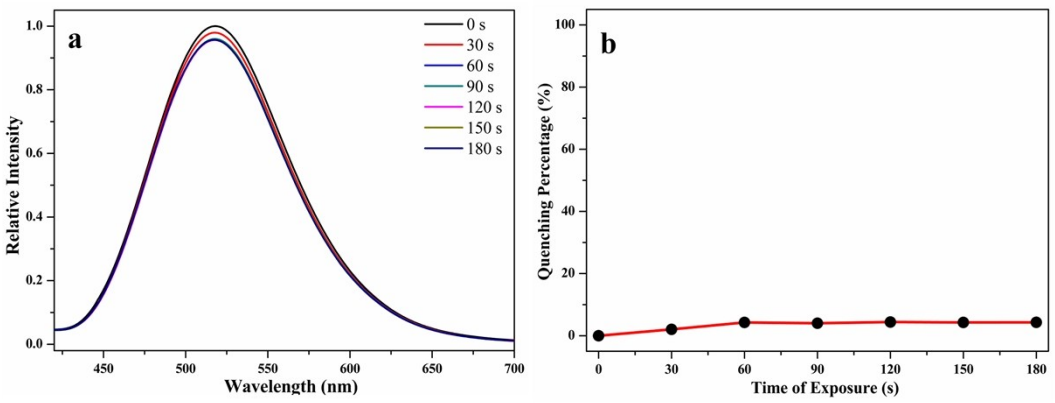

Fig. S22 Time-dependent photoluminescent spectra (a) and quenching percentage (b) of **1** to the *p*-AA vapor.

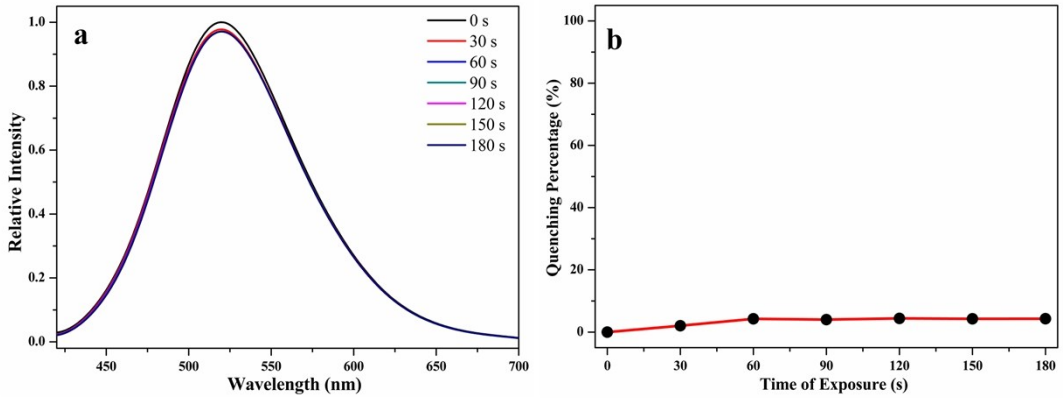

Fig. S23 Time-dependent photoluminescent spectra (a) and quenching percentage (b) of **1** to the A vapor.

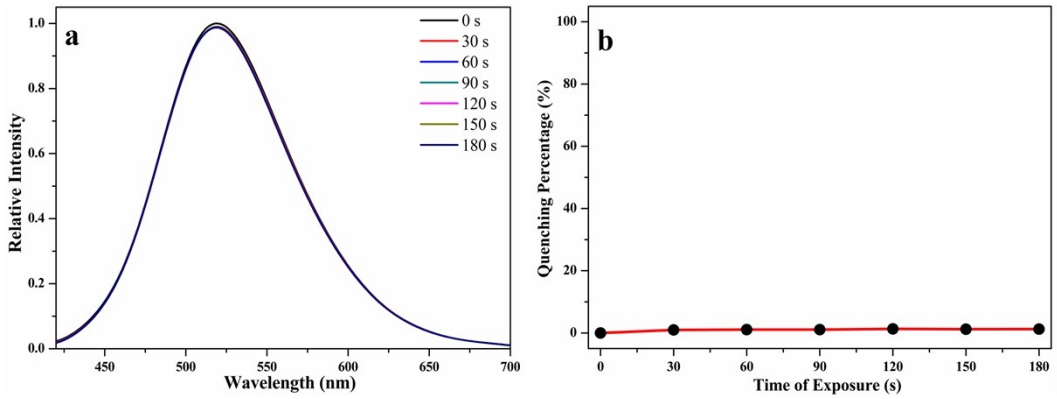

Fig. S24 Time-dependent photoluminescent spectra (a) and quenching percentage (b) of **1** to the NB vapor.

Under the same experimental conditions as compound **1**, the luminescence-quenching experiments were also performed with gradual addition of different aromatic analytes to Hbpba dissolved in

DMF (0.5 mg/mL). Corresponding results are shown in Fig. S25 and S26. It is found that, all the aromatic analytes can weaken the fluorescence intensity of Hbpba, however, the quenching efficiency (QE) conducted by Hbpba is different with compound **1**. For Hbpba-sensing, besides *p*-NA (85.58%) and *o*-NA (67.35%), *p*-AP also exhibits significant photoluminescence QE (46.31%), which is even higher than *m*-NA (24.64%). These results imply that superior sensitivity towards NA isomers would be strongly interfered by *p*-AP, and Hbpba-sensing is undesirable. When Hbpba coordinated to Zn ions, the resulting sensor of **1** exhibits highly sensitive and selective detection towards NA. In this case, compound **1** was used as a promising luminescent sensor for nitroaromatic detection.

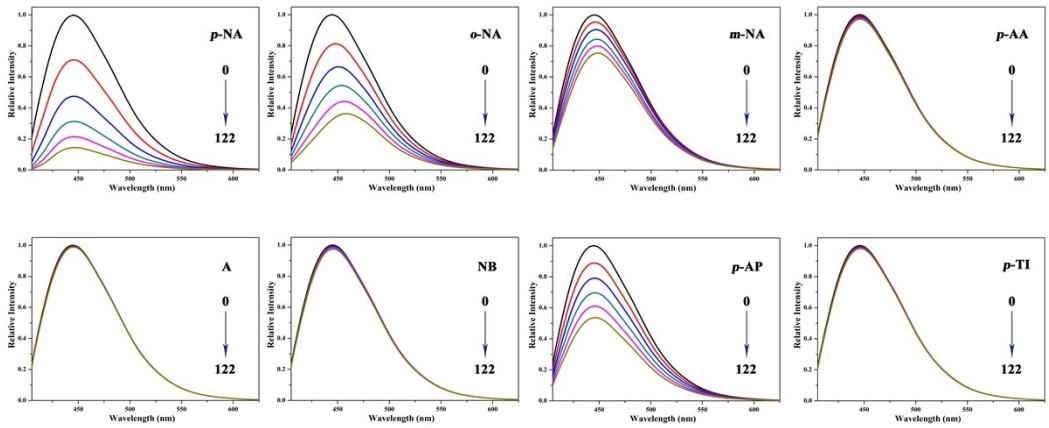

Fig. S25 Photoluminescent spectra of Hbpba in DMF treated with the different aromatic analytes concentration from 0 μM (black line) to 122 μM (dark yellow line) excited at 401nm.

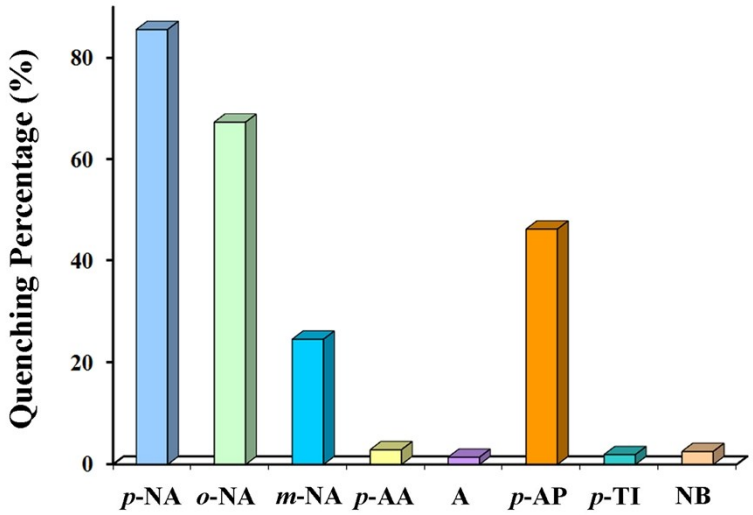

Fig. S26 Percentage of photoluminescence quenching of Hbpba upon addition of different aromatic analytes.

References

1 J. Wu, Y. Qu, L. Wang, L. Huang, Y. Rui, J. Cao and J. Xu, *Dyes and Pigments*., 2017, **136**, 175-181.

2 Y. Yang, K. Shen, J. Lin, Y. Zhou, Q. Liu, C. Hang, H. N. Abdelhamid, Z. Zhang and H. Chen, *RSC Adv*., 2016, **6**, 45475-45481.

3 M. J. Frisch, G. W. Trucks, H. B. Schlegel, G. E. Scuseria, M. A. Robb, J. R. Cheeseman, G. Scalmani, V. Barone, B. Mennucci, G. A. Petersson, H. Nakatsuji, M. Caricato, X. Li, H. P. Hratchian, A. F. Izmaylov, J. Bloino, G. Zheng, J. L. Sonnenberg, M. Hada, M. Ehara, K. Toyota, R. Fukuda, J. Hasegawa, M. Ishida, T. Nakajima, Y. Honda, O. Kitao, H. Nakai, T. Vreven, J. A. Montgomery, Jr., J. E. Peralta, F. Ogliaro, M. Bearpark, J. J. Heyd, E. Brothers, K. N. Kudin, V. N. Staroverov, R. Kobayashi, J. Normand, K. Raghavachari, A. Rendell, J. C. Burant, S. S. Iyengar, J. Tomasi, M. Cossi, N. Rega, J. M. Millam, M. Klene, J. E. Knox, J. B. Cross, V. Bakken, C. Adamo, J. Jaramillo, R. Gomperts, R. E. Stratmann, O. Yazyev, A. J. Austin, R. Cammi, C. Pomelli, J. W. Ochterski, R. L. Martin, K. Morokuma, V. G. Zakrzewski, G. A. Voth, P. Salvador, J. J. Dannenberg, S. Dapprich, A. D. Daniels, Ö. Farkas, J. B. Foresman, J. V. Ortiz, J. Cioslowski, D. J. Fox, Gaussian 09, Revision A.1, Gaussian, Inc., Wallingford CT, 2009.